

First principles modeling of the interface between a solid state lithium thiophosphate electrolyte and a lithium metal anode

N. A. W. Holzwarth

Department of Physics, Wake Forest University, Winston-Salem, NC, 27109, USA

Introduction

Recently, there has been good progress in improving the conductivity and stability of lithium thiophosphate solid electrolytes such as Li_3PS_4 . [1] For a variety of interface configurations, computer modeling studies show that Li_3PS_4 surfaces are structurally and chemically altered by the presence of Li metal. On the other hand, experiments have shown [1] that an electrochemical cell of $\text{Li}/\text{Li}_3\text{PS}_4/\text{Li}$ can be cycled many times. One possible explanation of the apparent stability of the Li_3PS_4 electrolyte/Li metal interface, is that a stable thin buffer layer is formed during the first few cycles. In order to computationally explore this possibility, we modeled a thin film buffer layer of Li_2S on a surface of Li_3PS_4 . Using first principles techniques described in previous work, [2] stable electrolyte-buffer layer configurations were found. Results for the idealized configurations indicate that a thin film of Li_2S can provide a protective buffer layer to stabilize the interface between the Li_3PS_4 electrolytes and Li metal anodes.

Computational Methods

Computational methods used in this work are based on density functional theory, [3] using the projector augmented wave (PAW) [4] formalism. The PAW basis and projector functions were generated by the *atompaw* [5] code and used in both the *abinit* [6] and *quantum espresso* [7] packages. The exchange-correlation functional was the local density approximation (LDA). [8] The choice of the LDA functional was made on the basis of previous investigations [9] of Li_3PO_4 .

Computational Methods – continued

In previous work, we showed that while the LDA results systematically underestimate the size of the lattice parameters, the LDA results for high frequency phonon frequencies were in much better agreement with experiment than those obtained using the generalized gradient approximation [10] (GGA) functional. We also showed that the fractional atomic coordinates were very similar to experiment and that the energetics associated with Li^+ migration were computed to be very similar using either exchange correlation functional.

For analyzing formation energies and other perfect crystal properties, calculations were performed with plane wave expansions of the wavefunction including $|\mathbf{k} + \mathbf{G}|^2 \leq 64 \text{ bohr}^{-2}$ and sampling of the Brillouin zone at least as dense as $10^{-3} \text{ bohr}^{-3}/\text{k-point}$. In fact, structural parameters and relative energies were well converged with a smaller number of plane waves ($|\mathbf{k} + \mathbf{G}|^2 \leq 49 \text{ bohr}^{-2}$) and a sparser Brillouin zone sampling of $0.02 \text{ bohr}^{-3}/\text{k-point}$, so that simulations requiring larger supercells could be well approximated using these less stringent convergence parameters. Surface properties were modelled using a slab geometry within supercells containing an additional 10 bohr representing the vacuum region. Interface properties with Li were modeled using a periodic array of electrolyte and metallic slabs. The volume available for the lithium slabs was determined by constrained optimization.

Computational Methods – continued

The partial densities of states $N^a(E)$ were calculated as programmed in the *abinit*[6] package,[11] based on an expression of the form

$$N^a(E) = \sum_{n\mathbf{k}} W_{n\mathbf{k}} Q_{n\mathbf{k}}^a \delta(E - E_{n\mathbf{k}}). \quad (1)$$

In this expression a denotes an atomic site, $W_{n\mathbf{k}}$ denotes the Brillouin zone sampling and degeneracy weight factor for band index n and wave vector \mathbf{k} , $E_{n\mathbf{k}}$ denotes the band energy. For each eigenstate $n\mathbf{k}$, the local density of states weight factor $Q_{n\mathbf{k}}^a$ for atomic site a is given by the charge within the augmentation sphere of radius r_c^a which can be well approximated by

$$Q_{n\mathbf{k}}^a \approx \sum_{n_i l_i m_i n_j} \langle \tilde{\Psi}_{n\mathbf{k}} | p_{n_i l_i m_i}^a \rangle \langle p_{n_j l_j m_j}^a | \tilde{\Psi}_{n\mathbf{k}} \rangle q_{n_i l_i; n_j l_j}^a \delta_{l_i l_j}, \quad (2)$$

in terms of the radial integrals

$$q_{n_i l_i; n_j l_j}^a \equiv \int_0^{r_c^a} dr \varphi_{n_i l_i}^a(r) \varphi_{n_j l_j}^a(r). \quad (3)$$

In these expressions, $|\tilde{\Psi}_{n\mathbf{k}}\rangle$ represents the pseudo-wavefunction and $|\tilde{p}_{n_i l_i m_i}^a\rangle$ represents the PAW atomic projector function which is localized within the augmentation sphere about the atomic site a and $n_i l_i m_i$ denote the radial and spherical harmonic indices of the projector function.[4] The function $\varphi_{n_i l_i}^a(r)$ represents an all-electron radial basis function. The augmentation radii used in this work are $r_c^{\text{Li}} = 1.6$, $r_c^{\text{O}} = 1.2$, $r_c^{\text{P}} = 1.7$, and $r_c^{\text{S}} = 1.7$ in bohr units.

Visualizations were constructed using the *XCrySDEN*[12] and *VESTA*[13] software packages.

Electrolyte-metal interface models

Bulk Li_3PS_4 is known[14,15] to crystallize in at least 2 different structures as does the similar lithium phosphate material Li_3PO_4 . [16] We have examined both the $Pnma$ and the $Pmn2_1$ structured materials and find qualitatively similar results. For simplicity only the results for the $Pmn2_1$ structured materials are presented here. According to the nomenclature of Ref. [15] and [16] the $Pmn2_1$ phases of lithium phosphate and lithium thiophosphate are given as $\beta\text{-Li}_3\text{PO}_4$ and $\gamma\text{-Li}_3\text{PS}_4$. For both of these materials the [010] surface has lowest energy.

Li / Li₃PO₄ / Li interface

The relaxed structure of a 2-layer [010] slab of $\beta\text{-Li}_3\text{PO}_4$ together with several layers of pure Li is illustrated in Fig. 1. The structure shows a physically well-defined interface between the electrolyte and the Li layers representing the anode material. We find that the qualitative results are insensitive to the details of the structure of the Li slab, provided that the volume is adjusted to accommodate the amount of Li ($\approx 18 \text{ \AA}^3$ per Li atom).

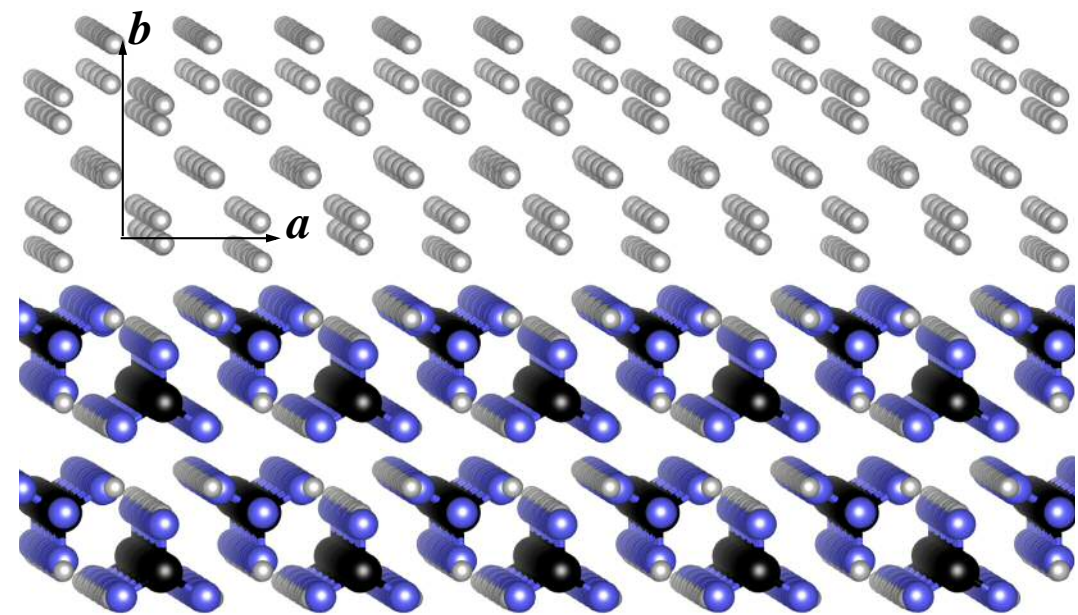


FIG. 1: Ball and stick representation of optimized structure of an ideal [010] slab of $\beta\text{-Li}_3\text{PO}_4$ with several layers of Li. The supercell contains 4 formula units of $\beta\text{-Li}_3\text{PO}_4$ and 14 Li atoms. The Li, P, and O sites are depicted with gray, black, and blue balls, respectively.

While Fig. 1 shows a physically well-defined interface between the Li₃PO₄ electrolyte and Li anode material, real battery materials have additional consideration. In addition to the physical stability of the interface, the partial density of states analysis suggests that the interface is chemically stable as well. The partial density of states of this system is shown in Fig. 2. Here it is seen that the metallic states are energetically above the occupied electrolyte states. In this supercell the metallic states are separated from the electrolyte states with a small energy gap of 0.3 eV. This property is common to all of the lithium metal interfaces with lithium phosphate surfaces that we have studied.

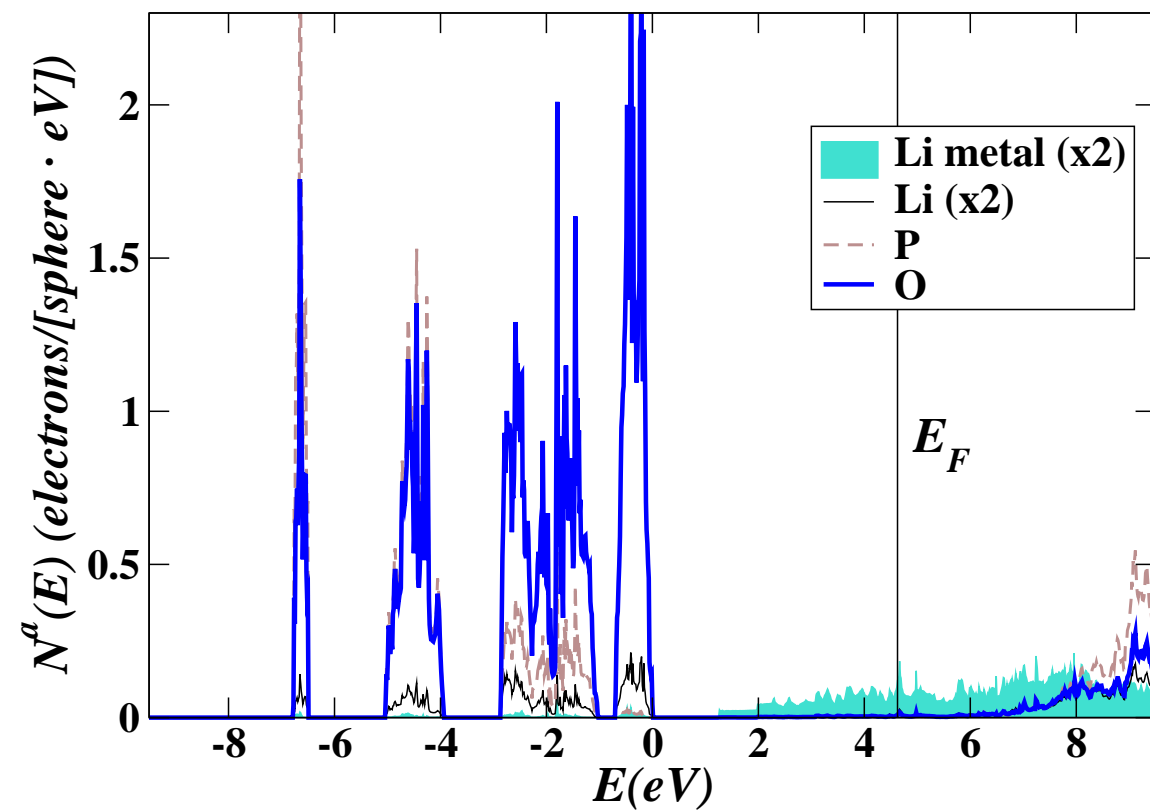


FIG. 2 Partial density of states plot of the β -Li₃PO₄ electrolyte in the Li presence of Li layers shown in FIG. 1. The energy scale for the plot was adjusted to the top of the filled valence band of the β -Li₃PO₄ layer. The weight factors for the partial densities of states are given by Eq. (2) for each type of atomic site a , averaged over sites of the same type.

In contrast with the lithium phosphate materials, models of ideal Li₃PS₄ surfaces were found to be structurally (and chemically) altered by the presence of Li metal atoms as shown in Fig. 3. In this example, a 2-layer [010] slab of γ -Li₃PS₄ is prepared in vacuum and one Li atom per formula unit is added to the supercell (Fig. 3(a)). After the system is allowed to relax (Fig. 3(b)), the thiophosphate ions at the surface layer are found to be significantly altered. The (meta-)stable structure shown in Fig. 3(b) was generated by the optimization algorithm of the *Quantum Espresso* software[7] and may not represent a physically realizable structure. On the other hand, the qualitative result that metallic Li breaks the S–P bonds at a surface of γ -Li₃PS₄ is a clear conclusion of this analysis. We observed similar behavior for simulations of slabs of β -Li₃PS₄ in the presence of Li metal as well.

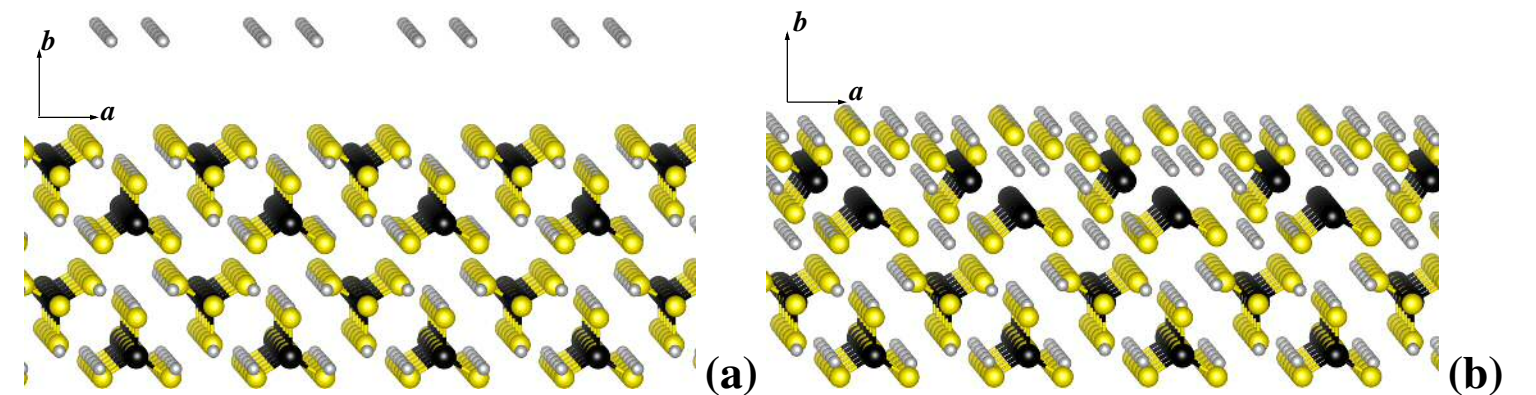


FIG. 3 Ball and stick representation of Li₃PS₄ surfaces with Li, P, and S sites depicted with gray, black, and yellow balls, respectively. **a:** Ideal [010] slab of γ -Li₃PS₄ with initial position of Li atoms. The supercell contains 4 formula units of γ -Li₃PS₄ and four Li atoms. **b:** Relaxed structure of configuration **a**.

On the other hand, it has been shown[1] that Li₃PS₄ can be cycled many times with a Li metal anode. One possible explanation of the apparent stability of the Li₃PS₄ electrolyte is that a stable thin buffer layer containing Li₂S is formed during the first few cycles.[17] We have explored this possibility computationally.

In order to model the effects of a Li₂S buffer layer on a Li₃PS₄ electrolyte, we added a 2-layer “thin film” of Li₂S on both sides of the γ -Li₃PS₄ slab as shown in Fig. 4(a). The “thin film” of cubic Li₂S was oriented in its non-polar [110] direction. The optimized lattice constants for the composite slab are within 0.1 Å of those computed for vacuum conditions. Two Li₂S groups are accommodated along the “a” axis with a compression of approximately 0.3 Å, while one Li₂S group is accommodated along the “c” axis with an expansion of approximately 0.4 Å in comparison to cubic Li₂S. While the construction of this buffer layer is not unique, the structure was found to be very stable with a binding energy of -0.9 eV/(reference unit) compared with the separated units calculated in the same supercell. (In this case the reference unit is Li₃PS₄ plus 2Li₂S.) Now, when Li metal is introduced in the vicinity of the buffered Li₃PS₄ electrolyte, stable configurations are achieved as shown in Fig. 4(b).

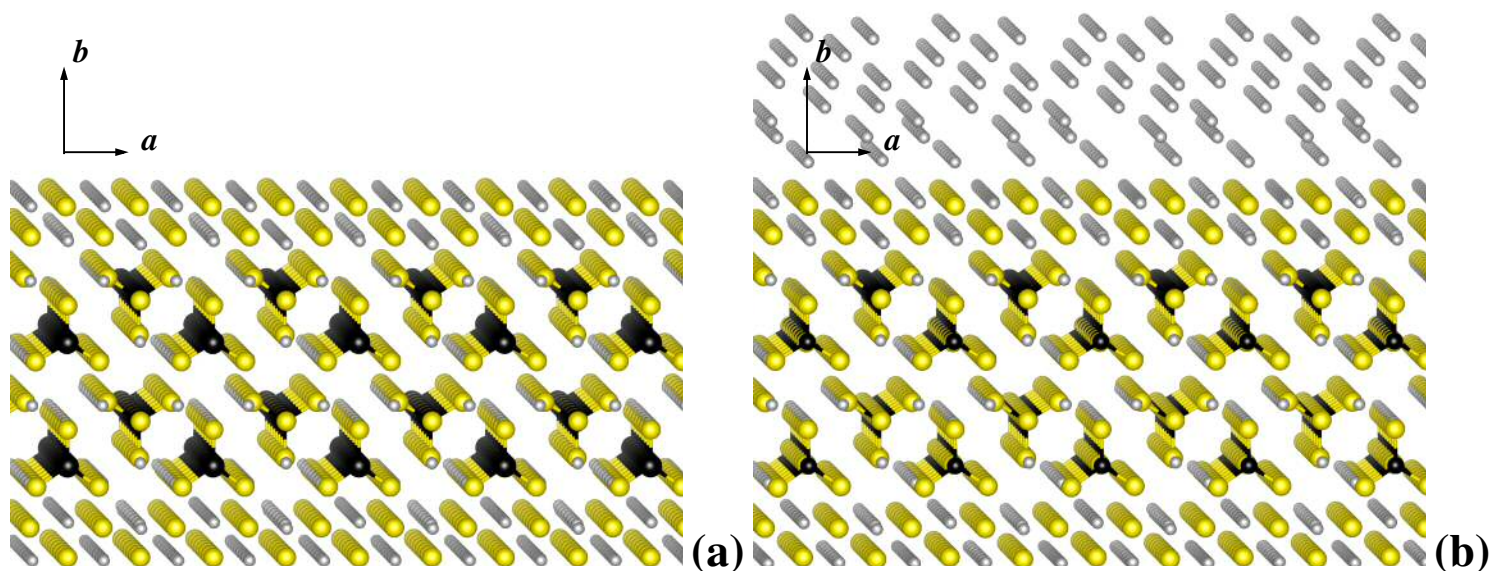


FIG. 4 a: Relaxed structure of a [010] slab of γ -Li₃PS₄ with buffer layers of Li₂S. The supercell contains 4 units of Li₃PS₄ and 8 units of Li₂S. **b:** Relaxed structure of buffered electrolyte shown in (a) with the addition of 14 Li atoms in the supercell.

Investigating the buffered electrolyte system further, we determined the partial density of states of the system as shown in Fig. 5. Here we see that, while the energy distribution of the electrolyte and anode states is not as well separated as in the lithium phosphate case, most of the metallic spectrum lies energetic above the electrolyte and buffer states.

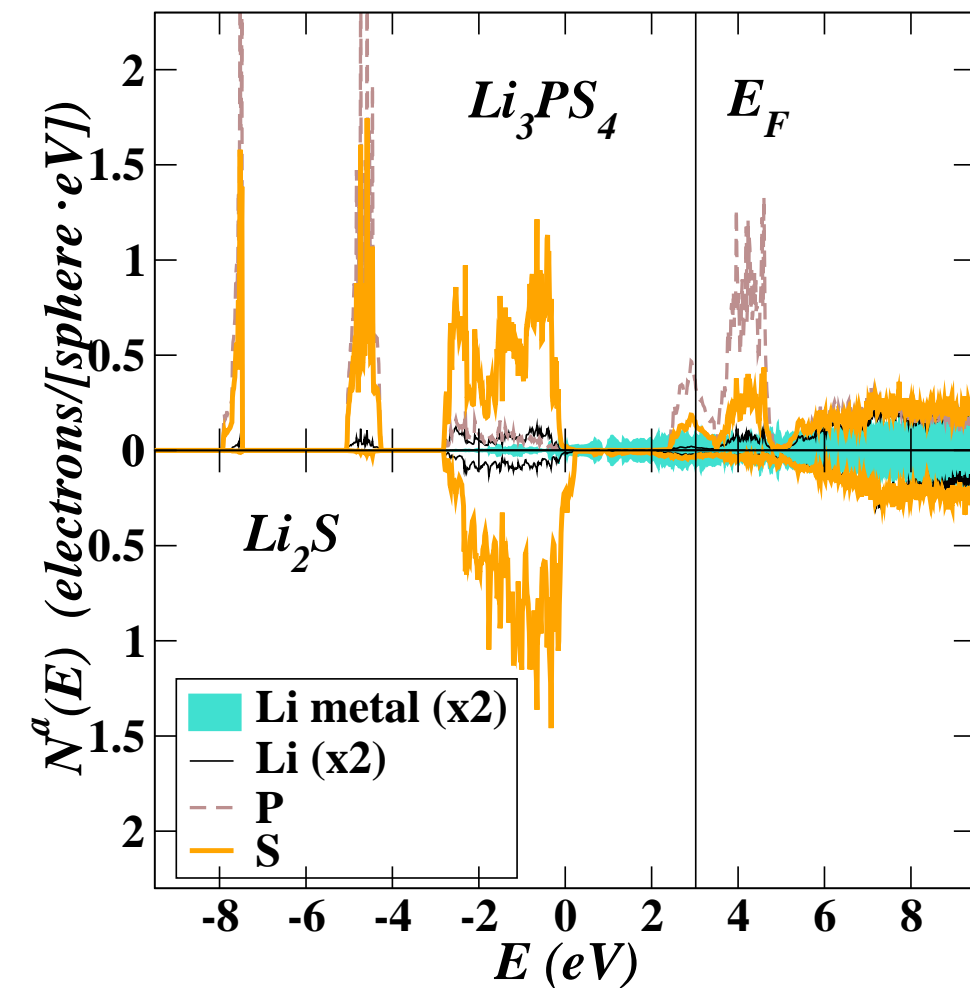


FIG. 5 Partial density of states plot of γ -Li₃PS₄ electrolyte, buffered with Li₂S in the Li presence of Li layers as shown in Fig. 4(b). The upper panel shows the states associated with the γ -Li₃PS₄ layers and the lower panel shows the states associated with the Li₂S buffer layers. Both panels show the contributions from the metallic Li layer. The energy scale for the plot was approximately adjusted to the top of the filled valence band of the γ -Li₃PS₄ layer. The weight factors for the partial densities of states are given by Eq. (2) for each type of atomic site a , averaged over sites of the same type.

Summary and Conclusions

Solid electrolyte technology was pioneered at Oak Ridge National Laboratory with the development of LiPON for use in thin film micro-batteries.[18] Our simulations of idealized interfaces of Li_3PO_4 with Li metal shown in Fig. 1 and the corresponding densities of states shown in Fig. 2 are consistent with the experimental findings the lithium phosphate is very stable in the presence of Li metal at voltages as high as 5.5 V and at elevated temperatures. LiPON differs from idealized $\beta\text{-Li}_3\text{PO}_4$ materials because of its disordered structure and the incorporation of N which serve to increase the ionic conductivity, but the physical and chemical stability is well represented by the idealized models.

In order for for solid electrolytes to meet the needs of high capacity battery technology, it is necessary for the conductivity to be increased by several orders of magnitude. A recent Nature Materials paper by researchers in Japan [19] has energized this effort with the development of a solid electrolyte having conductivities comparable to those of commercially available liquid electrolytes.

Summary and Conclusions – continued

One of the most stable solid electrolytes with increased conductivities compared with LiPON is $\beta\text{-Li}_3\text{PS}_4$. [1] By processing the material into nano porous form, the more conductive $\beta\text{-Li}_3\text{PS}_4$ structure was stabilized with respect to the lower energy form of $\gamma\text{-Li}_3\text{PS}_4$, and the nano porous form was also shown to have higher conductivity over previously studied bulk forms of $\beta\text{-Li}_3\text{PS}_4$. [20,15]

The results of our simulations illustrated in Fig. 3-5 show that even for an idealized structure of Li_3PS_4 , the stability issue is non-trivial. We have shown that the pure Li_3PS_4 surface is unstable in the presence of Li metal, but that a very thin buffer layer of Li_2S can protect the surface from degradation. In the experimental processing, it is possible that this buffer layer forms naturally during the first few cycles of battery operation, much like the SEI layer forms in liquid electrolytes. Further work is needed to study how this layer effects the overall conductivity and performance of the electrolyte.

Acknowledgements

Nicholas Lepley contributed to this project. The work was supported by NSF grant DMR-1105485 and by the Wake Forest University DEAC computer cluster. Helpful discussions on various aspects of this work from colleagues at Oak Ridge National Laboratory are gratefully acknowledged. In particular Nancy Dudney and Chengdu Liang provided experimental advice and Paul Kent and Gopi Krishna Phani Dathar discussed computational and modeling issues.

Bibliography

- [1] Z. Liu, W. Fu, E. A. Payzant, X. Yu, Z. Wu, N. J. Dudney, J. Kiggans, K. Hong, A. J. Rondinone, and C. Liang, *J. Am. Chem. Soc.* **135**, 975 (2013).
- [2] N. A. W. Holzwarth, N. D. Lepley, and Y. A. Du, *J. Power Sources* **196**, 6870 (2011).
- [3] P. Hohenberg and W. Kohn, *Physical Review* **136**, B864 (1964); W. Kohn and L. J. Sham, *Physical Review* **140**, A1133 (1965).
- [4] P. E. Blöchl, *Phys. Rev. B*, **50**, 17953 (1994).
- [5] A. R. Tackett, N. A. W. Holzwarth, and G. E. Matthews, *Computer Physics Communications* **135**, 348 (2001). Available from the website <http://pwpaw.wfu.edu>.
- [6] X. Gonze *et al.* (32 authors) *Computer Physics Communications* **180**, 2582 (2009). Available from the website <http://www.abinit.org>.
- [7] P. Giannozzi *et al.* (32 authors) *J. Phys.: Condens. Matter* **21**, 394402 (2009). Available from the website <http://www.quantum-espresso.org>.
- [8] J. P. Perdew and Y. Wang, *Phys. Rev. B* **45**, 13244 (1992).

Bibliography – continued

- [9] Y. A. Du and N. A. W. Holzwarth, *Phys. Rev. B* **81**, 184106 (2010).
- [10] J. P. Perdew, K. Burke, and M. Ernzerhof, *Phys. Rev. Lett.* **77**, 3865 (1996), erratum – *Phys. Rev. Lett.* **78**, 1396 (1997).
- [11] Similar capabilities are currently being implemented into the *quantum espresso* package.
- [12] A. Kokalj, *Journal of Molecular Graphics and Modelling* **17**, 176 (1999). Available from the webpage www.xraysden.org.
- [13] K. Momma and F. Izumi, *Applied Crystallography* **44**, 1272 (2011). Available from the webpage <http://jp-minerals.org/vesta/en/>.
- [14] R. Mercier, J. - P. Malugani, B. Fahyst, and G. Robert, *Acta Cryst.* **B38**, 1887 (1982).
- [15] K. Homma, M. Yonemura, T. Kobayask, M. Nago, M. Hirayama, and R. Kanno, *Solid State Ionics* **182**, 53 (2011).
- [16] C. Keffer, A. Mighell, F. Mauer, H. Swanson, and S. Block, *Inorganic Chemistry* **6**, 119 (1967).
- [17] C. Liang and N. J. Dudney, private communication.
- [18] N. J. Dudney, *Interface* **17**(3), 44 (2008).
- [19] N. Kamaya, K. Homma, Y. Yamakawa, M. Hirayama, R. Kanno, M. Yonemura, T. Kamiyama, Y. Kato, S. Hama, K. Kawamoto, and A. Mitsui, *Nature Materials* **10** 682 (2011).
- [20] M. Tachez, J. -P. Malugani, R. Mercier, and G. Robert, *Solid State Ionics* **14**, 181 (1984).